The potential use of N-octanoyl-dopamine (NOD) in organ transplantation

Wedel, Johannes

9

N-octanoyl-dopamine attenuates the development of transplant vasculopathy in rat aortic allografts via smooth muscle cell protective mechanisms

Johannes Wedel
Maximilia C. Hottenrott
Benito A. Yard
Jan-Luuk Hillebrands

submitted.

Abstract

Transplant vasculopathy (TV) is a major cause for late graft loss after cardiac transplantation. Endothelial damage and T cell infiltration play a pivotal role in the development of TV. Since N-octanoyl-dopamine (NOD) inhibits vascular inflammation and suppresses T cell activation *in vitro*, we here tested the hypothesis that NOD-treatment ameliorates TV.

Aortic grafts were orthotopically transplanted in the Dark Agouti to Brown Norway strain combination. Recipient rats were treated with either NOD or saline administered via osmotic minipumps. Histology was performed on grafts explanted 2 and 4 weeks after transplantation to assess the degree of TV, inflammation, number of (proliferating) αSMA$^+$ neointimal cells. *In vitro* analysis of human aortic smooth muscle cells (haSMC) were performed to test the effect of NOD on haSMC proliferation (WST-1 assay), cell cycle (flow cytometry and qPCR), and cytokine-induced apoptosis (flow cytometry).

Allografts from vehicle-treated recipients developed neointimal lesions predominantly consisting of αSMA expressing cells. NOD-treatment significantly reduced neointima formation and reduced relative and absolute numbers of αSMA$^+$ SMC. *In situ*, Ki67 expression (proliferation) in SMC was not influenced by NOD. T cell (CD3) and macrophage (CD68) infiltration was similar in vehicle- and NOD-treated rats. *In vitro*, NOD inhibited proliferation of haSMC by causing a G1-arrest as determined by FACS and qPCR. NOD protected haSMCs from TNF-α-induced apoptosis.

This study identified NOD as potential treatment modality to attenuate TV. Our *in vitro* data clearly support a vasculoprotective effect of NOD by reducing SMC proliferation and inflammation-induced apoptosis.

Introduction

Organ transplantation has become the treatment of choice for end-stage organ failure. While in the early years acute rejections were a major cause for graft loss, with the introduction of calcineurin inhibitors (CNI) acute rejection episodes became clinically manageable and resulted in an overall improved 1-year graft survival [1]. Despite this improvement, chronic transplant loss was not positively affected by CNI; use of CNI was rather recognized as a risk factor for chronic graft loss based on several adverse effects [2,3]. Particularly in cardiac allografts, chronic graft loss is accompanied by transplant vasculopathy (TV) [4] which is characterized by intimal thickening, medial smooth muscle cell (SMC) apoptosis and intimal SMC proliferation. Even though much scientific efforts have been put in prevention of TV, there is no adequate treatment currently available [5] and thus prevention of TV remains a scientific challenge in transplantat medicine. Damage of the endothelium is now well recognized as an important initial step in the development of TV. Both immunological and non-immunologic factors contribute to vascular damage which may occur as a consequence of organ preservation, ischemia/reperfusion (I/R), (subclinical) cellular and humoral rejection episodes and virus infections. Also the traditional cardiac risk factors, *e.g.* dyslipidemia and hypertension, may cause endothelial cell injury [6]. Irrespective of the cause of endothelial damage, leukocytes are mostly recruited to these sites of damage and infiltrate into the subendothelial space causing vascular inflammation [7,8]. Platelets may become activated at these sites and start to release procoagulant and proinflammatory factors thereby perpetuating inflammation [9,10] and recruitment of progenitor cells [11,12]. In addition, several studies clearly showed a positive correlation between endothelial injury and progenitor cell recruitment [13]. It is believed that the hematopoietic progenitor cells proliferate *in situ*, dedifferentiate into smooth muscle-like cells and secrete extracellular matrix proteins which form a neointima (NI) [14-19]. Infiltrated alloreactive T cells are also involved in TV as they may cause medial SMC apoptosis via production of TNF-α or INF-γ [20-23]. Both cytokines will further activate surrounding endothelial cells with subsequent leukocyte recruitment and platelet activation. Therefore, strategies that aim to break this vicious cycle hold the promise of preventing TV. Indeed it has been shown that platelet inhibition results in improved glomerular filtration rates (GFR) after 2 years of treatment of renal allograft recipients [24]. Other experimentally effective strategies that have shown to affect TV are amongst others based on limiting leukocyte recruitment [25],

inhibition of intimal smooth muscle cell proliferation [26] or transcriptional inhibition of inflammatory mediators [27].

In a prospective randomized multicenter trial we have shown that donor treatment with low-dose dopamine has a salutary effect on immediate kidney graft function [28]. In a subgroup analysis this was translated into a better graft survival for recipients who obtained a renal allograft with prolonged cold preservation time. Graft survival was also improved in heart allograft recipients [29] but did not affect outcome after liver transplantation [28]. Based on *in vitro* experiments, we have postulated that the protective effect of dopamine is independent of its hemodynamic action and requires the redox active catechol structure [30]. Moreover, we have shown that conjugation of n-octanoic acid to the amine side chain of dopamine, which likely impairs adrenergic and dopaminergic receptor engagement, results in a far more protective compound [31]. N-octanoyl-dopamine (NOD) not only protects cells and tissues against prolonged hypothermic preservation [31], it also strongly inhibits platelet function *ex vivo* [32], prevents NF-κB activation *in vitro* [33] and inhibits T cell activation and proliferation [34]. *In vivo*, we showed that NOD also mitigates ischemia-induced acute kidney injury [35]. In keeping with the notion that the endothelium, platelets and T cells play pivotal roles in TV development, the present study was conducted to assess the influence of NOD on development of TV *in vivo*.

Materials and Methods

N-octanoyl-dopamine synthesis

NOD was synthesized from commercially available precursors as previously described [31]. Briefly, octanoic acid was dissolved in tetrahydrofuran and N-ethyldiisopropylamine before conversion to their mixed anhydride by the reaction with ethyl chloroformate. For coupling the crude mixed anhydride and dopamine hydrochloride were dissolved in N,N-dimethylformamide in the presence of diisopropylamine. Sodium hydrogen carbonate and sodium sulfite were added and after evaporation of the solvent the product was obtained. The product was purified by two-fold recrystallization from dichloremethane which was proved by thin layer chromatography. Samples were investigated by ^{1}H-NMR spectroscopy (Bruker AC250) and yielded spectra in accordance with the expected structure.

Rats

Male Dark Agouti (DA) and Brown Norway (BN) rats were obtained from Janvier (Saint-Berthevin, France). Rats, weighting 230-270 g, were kept under clean conventional conditions and were fed standard rat chow and tapped water *ad libitum*. All animals received humane care in compliance with the 'Principles of Laboratory Animal Care' formulated by the National Society for Medical Research and the 'Guide for the Care and Use of Laboratory Animals' prepared by the Institute of Laboratory Animal Resources and published by the National Institutes of Health (NIH Publication No. 86-23, revised 1996), and the Dutch Law on Experimental Animal Care. Experiments were approved by the animal ethics committee of the University of Groningen (DEC 6624B).

Experimental groups

To study the influence of NOD on TV development, orthotopic aortic transplantation from DA to BN rats was performed. All recipient rats underwent simultaneous implantation of osmotic minipumps s.c. (2x [2ML4, 2.5µl/h] for 4 weeks follow-up or 1x [2ML2, 5 µl/h] for 2 weeks follow-up) delivering either NOD (55.8 µg/h) or vehicle (2.5% Tween80 in 0.9% NaCl) via an i.v. cannula in the external jugular vein as we recently described [36]. Rats were sacrificed after 2 or 4 weeks after transplantation and grafts were removed and processed for histological analyses as described below.

Aorta transplantation

Aortic allografts (10-12 mm) were transplanted as described previously [37]. Briefly, both donor and recipient rats received inhalation anesthesia (2% isofluran/O_2, flow 0.5 l/min). The abdominal aorta between the left renal artery and the bifurcation was removed from the donor rat and perfused with saline to remove blood cells. After 1 hour of cold storage in 0.9% saline at 4°C, the aortic graft was orthotopically transplanted into the recipient via end-to-end anastomosis using 9-0 nylon suture. Total warm ischemic time was consistently 25 minutes. Recipient rats received 0.05 mg/kg buprenorphine during surgery and at days 1 and 2 post-transplantation. No anti-rejection therapy was administered.

Quantitation of transplant vasculopathy

Grafts removed at autopsy were fixed in formalin and embedded in paraffin. Tissue sections (3 µm) were taken from the center of each graft and were stained according Van Gieson to visualize elastin fibers. Slides were scanned on a digital slide scanner (ScanScope CS2) and quantitated using ImageScope 11.2 (both Aperio, Vista, USA). Surface neointima was quantified in nine sections from each graft: three sections cut at the center of the graft, and three sections cut 500 µm and 1000 µm distant hereof. Surface area NI was measured in 9 sections by subtracting lumen area from internal elastic lamina area. NI surface was normalized by dividing NI surface area by media surface area. For each graft the mean of all 9 sections was calculated.

Neointimal SMC proliferation in situ

To detect proliferating cells in aortic allografts (harvested 4 weeks after transplantation), immunohistochemistry for Ki67 and α-smooth muscle actin (αSMA) expression was performed on 3 µm sections from formalin-fixed paraffin embedded tissue. Heat-induced epitope retrieval (HIER) was performed in 10 mM citric acid (pH 6.0) for 15 min followed by endogenous peroxidase blockade using 0.3% H_2O_2 in PBS. After rinsing in PBS, sections were incubated with rabbit-anti-human-Ki67 polyclonal antibody (clone NCL-Ki67p, Novocastra, Leica, Rijswijk, The Netherlands) for 1 hour. After rinsing in PBS sections were sequentially incubated with goat-anti-rabbit-HRP and rabbit-anti-goat-HRP (both Dako, Heverlee, Belgium). HRP-activity was visualized using 3,3′-diaminobenzidine (DAB). Sections were then incubated for another hour with mouse-anti-human-αSMA monoclonal antibody (clone 1A4, mIgG2a,

Dako, Heverlee, Belgium) followed by incubation with rabbit-anti-mouse-alkaline phosphatase and stained using FastRed (Life Technologies, Bleiswijk, The Netherlands). Sections were counterstained with Mayer's haematoxylin, coverslipped in Kaiser's glycerol-gelatin, scanned on a digital slide scanner (Nanozoomer 2.0HT, Hamamatsu, Almere, Netherlands) and analyzed using HistoQuest software (version 3.5.3.0171, TissueGnostics, Vienna, Austria).

To assess inflammatory cell infiltration, allografts (removed 2 weeks after transplantation) were analyzed for $CD3^+$ and $CD68^+$ cells. To this end, 3 µm formalin-fixed and paraffin embedded sections were incubated with rabbit-anti-human-CD3 (clone IS503, Dako, Heverlee, Belgium) respectively mouse-anti-rat-CD68 (clone ED1, AbD serotec, Colmar, France) after HIER with 0.1 M Tris/HCl pH 9.0 at 80°C overnight. Staining was visualized with goat-anti-rabbit-HRP (CD3) respectively goat-anti-mouse-HRP (CD68) and rabbit-anti-goat-HRP (all from Dako, Heverlee, Belgium) using DAB and nuclei were counterstained with Mayer's hematoxylin. CD3 and CD68 positivity was analyzed using the positive pixel count v9 algorithm by ImageScope 11.2 (Aperio, Vista, USA). Data is expressed in positive pixel counts/area.

haSMC proliferation assay

Human aortic Smooth Muscle Cells (haSMC) were purchased from ScienCell (ScienCell Research Laboratories, Carlsbad, USA) and were seeded in 96-well flat bottom culture plates (1.5×10^4 cells/well) in SMC growth medium (ScienCell Research Laboratories, Carlsbad, USA) containing SMC growth supplement, 2% FBS, 100 U/ml penicillin and 100 U/ml streptomycin. Cells were allowed to attach for 24 hours, synchronized for 48 hours in starvation medium (*i.e.* SMC growth medium with 0.1% FBS without SMC growth supplement) and than followed by stimulation with SMC growth medium in the presence or absence of different concentrations of NOD (range 0-50 µM) for 48 hours. After adding WST-1 (Roche Diagnostics, Mannheim, Germany) for the last 2.5 hours of culture, colored formazan was quantified by an ELISA plate reader (Varioskan, Thermo Scientific, Erembodegem-Aalst, Belgium) at 450 nm. Results are expressed as absorbance at 450 nm ± SEM of six different experiments.

Cell cycle analysis

haSMC were seeded in 6-well flat bottom culture plates (5×10^5 cells/well) in SMC growth medium, allowed to attach for 24 hours, synchronized for 48 hours in starvation medium followed by stimulation with SMC growth medium in the presence or absence of different concentrations of NOD (range 0-50 μM) for 72 hours.

For nuclear staining, DRAQ5 (Biostatus, Shepshed, UK) was used at a final concentration of 10 μM according to the supplier's protocol. Fluorescence was assessed on a FACS Calibur flow cytometer (BD Biosciences, Breda, The Netherlands). At least 50,000 gated events were collected per sample and data was analyzed by Flowjo software (Tree Star, Ashland, USA).

For PCR analysis, total RNA was isolated using Trizol reagent (Life Technologies, Rockville, USA) according to the supplier's protocol. DNase-treatment was carried out using RNase free DNase I (Ambion, Woodward, Austin, USA). 1 μg total RNA was reverse-transcribed into cDNA using the First Strand cDNA Synthesis Kit (Roche Diagnostic, Mannheim, Germany). 1 μl cDNA was diluted in 19 μl DEPC-treated water and stored at -20°C until use. qPCR was performed on a StepOne real-time PCR (Life Technologies, Darmstadt, Germany) using TaqMan universal PCR master mix AmpErase UNG (Applied Biosystems, Darmstadt, Germany). The following Taqman assays were used: *AURKA* (Hs01582072_m1), *CCNA2* (Hs00996788_m1), *CCNB1* (Hs01030099_m1), *CDK1* (Hs00938777_m1) and *HPRT1* (Hs02800695_m1) (all Applied Biosystems, Darmstadt, Germany). Triplicate samples were run under the following conditions: initial denaturation for 10 min at 95°C followed by 40 cycles of 15 s at 95°C and 1 min at 60°C. The levels of gene expression in each sample were determined with the comparative cycle threshold method. PCR efficiency was assessed from the slopes of the standard curves and was found to be between 90% and 100%. Linearity of the assay could be demonstrated by serial dilution of all standards and cDNA. All samples were normalized for an equal expression of *HPRT1*.

haSMC apoptosis assay

haSMC were plated in 6-well culture plates in SMC growth medium at a density of 10^5 cells/well. Plated cells were allowed to attach for 24 hours, starved for an additional 24 hours and then stimulated with SMC growth medium in the presence or absence of different concentrations of NOD (0-50 µM) for varying time periods (3-24 hours). Positive control was obtained by adding 0.4 mM H_2O_2 to the culture for 4 hours. Cells were trypsinized, washed in PBS twice and stained with anti-Annexin V antibody and 7AAD (both from BioLegend, San Diego, USA) according the supplier's protocol. Fluorescence was assessed by flow cytometry and analyzed within 6 hours after finishing the staining protocol as described above.

Statistical analysis

Data is expressed as mean ± standard error of the mean (SEM). Statistical analysis was performed using Student's t-test with previous testing of normal distribution. A *p*-value of less than 0.05 was considered significant.

Results

Neointima formation in aortic grafts

NI formation was assessed 4 weeks after transplantation in the vehicle- and NOD-treated groups (Figure 1A). To this end, the total surface area of NI (Figure 1B) as well as the normalized NI (NI/M ratio) (Figure 1C) was measured by morphometric analysis. At termination, 4 out of 7 animals in the NOD group showed either disconnected pumps or catheters. Therefore, the NOD group

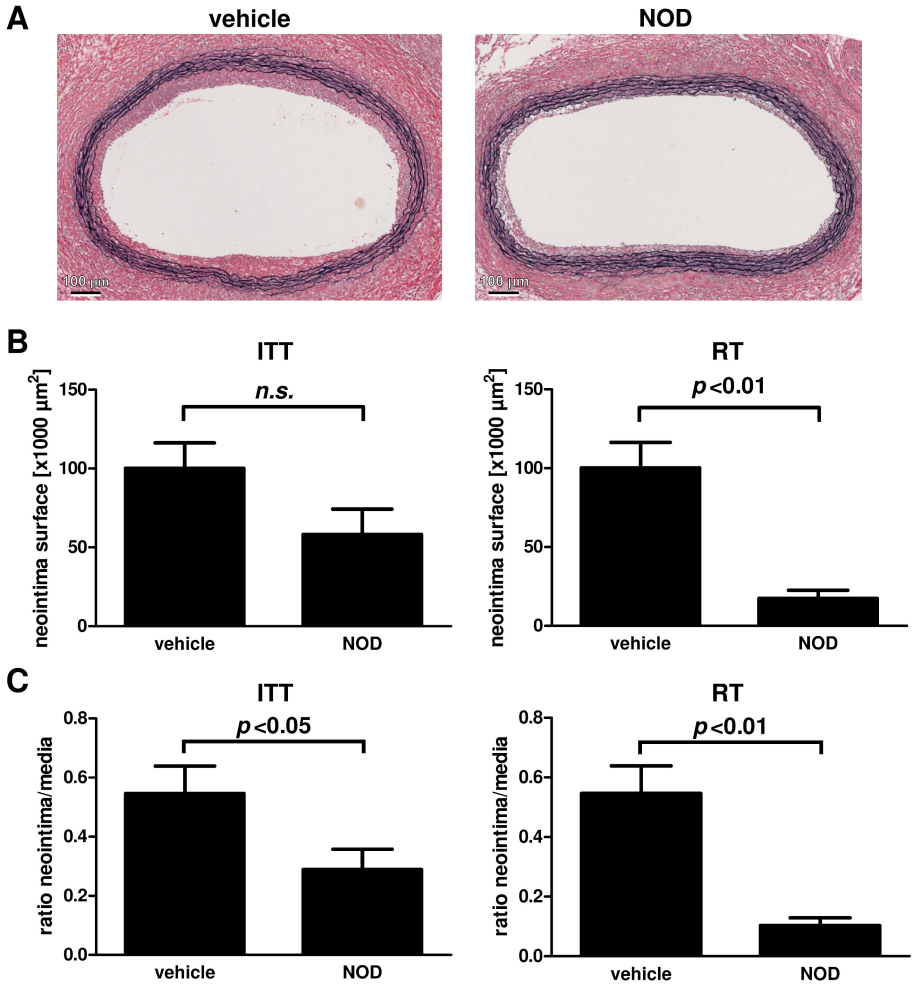

Figure 1: NOD inhibits neointima formation.

4 weeks after transplantation, grafts were stained according Verhoeff's van Gieson.

A: Representative aortas are depicted.

B: Surface of NI was assessed by subtracting the lumen area from inner border of elastin layer.

C: NI was normalized to aortic size by dividing NI area through medial area.

In *B* and *C* for each animal of each group serial section were made from the middle of the graft, and 500 and 1000 µm proximal hereof. For statistical analysis all sections were included (ITT: intention-to-treat; RT: received treatment).

was analyzed either as intention-to-treat (ITT) (n=7, including all animals) or as received treatment (RT) (n=3, excluding rats with anticipated administration failure because of observed disconnections at sacrifice). Since it is unknown when the pumps or catheter got disconnected during follow-up, we cannot estimate the amount of NOD delivered i.v. in these animals. We consider these animals therefore as suboptimally treated. NOD-treatment showed a trend towards reduced NI formation in the ITT analysis when expressed as the total NI surface (Figure 1B, left panel). When expressed as NI/M ratio, neointima formation was significantly reduced ($p<0.05$) in the NOD-treated rats (Figure 1C, left panel). After exclusion of the suboptimally treated rats, NOD-treatment showed a more pronounced reduction of NI formation as evidenced by a significant reduction in absolute NI surface area ($p<0.01$, Figure 1B, right panel) and NI/M ratio ($p<0.01$, Figure 1C, right panel). The suboptimally treated rats indeed displayed more pronounced NI formation (not shown).

α-Smooth muscle actin expression and neointimal SMC proliferation in situ

We next assessed if NOD-treatment reduces the number of neointimal αSMA expressing cells and if *in situ* proliferation of these cells was affected. To this end, we first validated in single stainings on paraffin sections the method and antibody specificity of anti-αSMA and anti-Ki67 antibodies (Figure 2A). The antibodies appeared to be highly specific without cross-reactivity of secondary and tertiary antibodies (not shown). Next we performed double staining on allograft sections. In contrast to isografts and non-transplanted aortas (not shown), in allografts a clear neointima was present composed of predominantly αSMA expressing cells (Figure 2B). In allografts αSMA expressing cells were hardly present anymore in the media, neither in vehicle- nor in NOD-treated rats (Figure 2B). Quantitative analysis for αSMA and Ki67 was performed using HistoQuest morphometric analysis (Figure 2C, right panel) in order to determine the total number of αSMA^+ neointimal cells as well as numbers of proliferating αSMA^+Ki67^+ neointimal cells. In contrast to the media, both αSMA and Ki67 expression were present in the NI (Figure 2C, left panel). While the ITT analysis already showed a trend towards a relative decrease in αSMA^+ cells in the NOD-treated group (*vs.* vehicle, Figure 2D, left panel), this was statistically significant ($p<0.05$) in RT analysis (Figure 2D, right panel). Total number αSMA^+ cells was significantly reduced in both analyses (Figure 2E), which is in line with reduced surface area NI as shown in *figure 1*. However, *in situ* proliferation of neointimal αSMA^+ cells,

as defined as αSMA⁺Ki67⁺ double positive cells, was not significantly different between the groups neither in ITT nor in RT analysis (Figure 2F). Similar results were obtained when using PCNA as proliferation marker (data not shown).

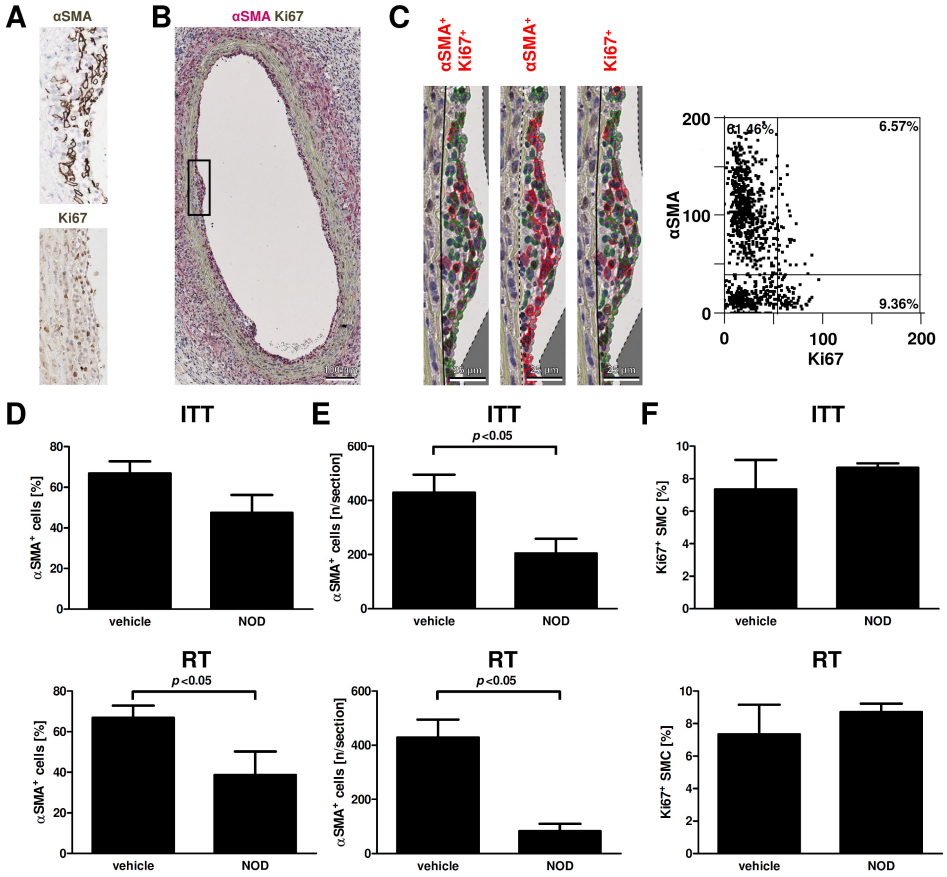

Figure 2: NOD reduces neointimal αSMA⁺ expression.

A double staining for αSMA (FastRed-red) and the proliferation marker Ki67 (DAB-brown) was performed.

A: Specificity of antibodies was demonstrated in single stainings.

B: A representative cross-section of a double stained graft is depicted. Note the loss of medial αSMA expression.

C: αSMA and Ki67 expression was analyzed by automated cell recognition software (HistoQuest, TissueGnostics, Vienna, Austria). To this end, counterstained nuclei were recognized and nuclear Ki67 (DAB-brown) and cytoplasmic αSMA (FastRed-red) of each cell was assessed. Cut-offs for positivity of markers were defined on dotplots (to the right) and correct gating was controlled using a backward gating strategy. Recognized cells are highlighted: cells positive for αSMA, Ki67 or both markers are encircled in red; negative cells in green.

D: αSMA⁺ cells on the basis of all neointimal cells (Ki67⁺ and Ki67⁻).

E: Absolute number of neointimal αSMA⁺ cells per section.

F: Quantification of *in situ* proliferating Ki67⁺αSMA⁺ cells.

D+E+F: For all grafts and for each group a total of 9 sections were evaluated. The sections were cut from the middle of the graft, and 500 and 1000 µm proximal hereof. For statistical analysis the mean of all sections was calculated (ITT: intention-to-treat; RT: received treatment).

Influence of NOD on T cell and macrophage infiltration in aortic grafts

Since we have previously shown that in this aortic transplant model for evaluation of mononuclear cell infiltration a two week follow-up was the optimal time point [37], recipients were also sacrificed after 2 weeks. Tissue sections were stained for infiltrating T cells and macrophages using anti-CD3 and anti-CD68 monoclonal antibodies, respectively (Figure 3).

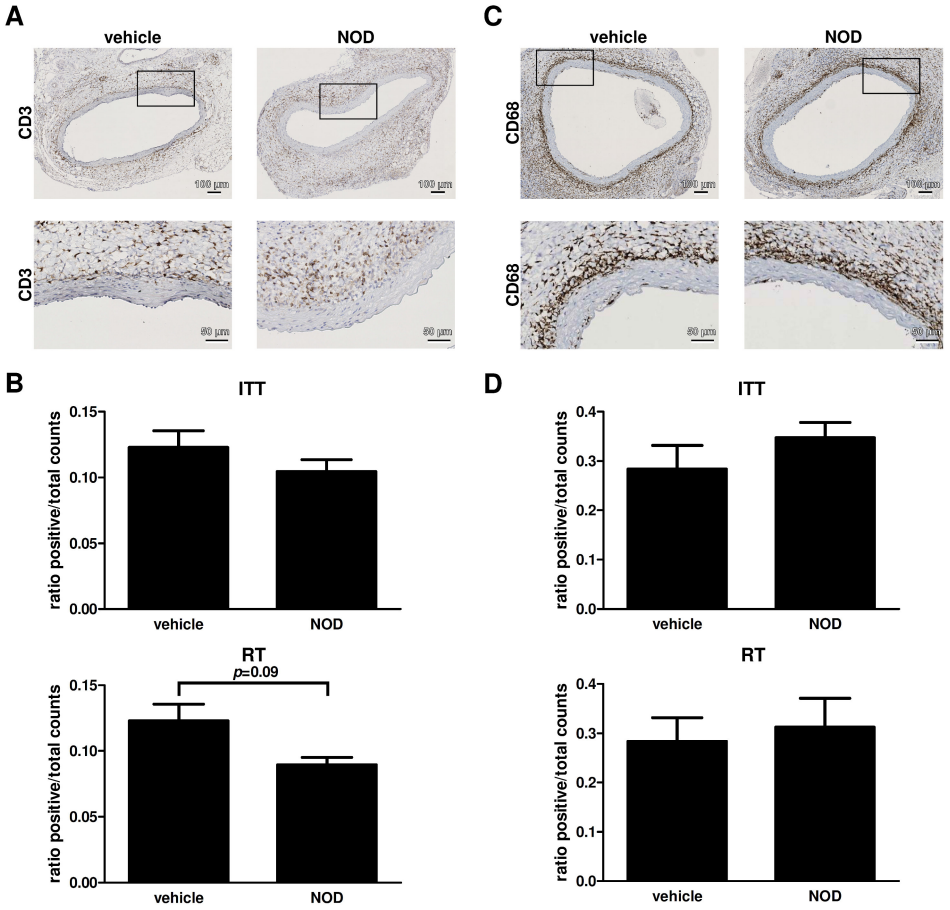

Figure 3: NOD does not reduce CD3⁺ T cell and CD68⁺ macrophage infiltration.

Inflammation of aortic allografts was assessed 2 weeks after transplantation by immunohistology using anti-CD3 and anti-CD68 (ED-1) antibodies.

A: Representative cross-sections of aortic allografts stained for T cells.

B: Quantification of infiltrated T cells.

C: Representative cross-sections of aortic allografts stained for macrophages.

D: Quantification of infiltrated macrophages.

B+*D*: Statistics were performed on 3 slides from the middle of the graft and 3 slides cut 500 µm further into the graft. Ratio of positive/total pixels of the whole section, containing NI, media and adventitia but excluding surrounding tissue, was assessed (ITT: intention-to-treat; RT: received treatment).

Whereas T cells ($CD3^+$) were predominantly found in the adventitia (Figure 3A), macrophages were present in both the adventitia and the subendothelial layer (Figure 3C). No difference in the degree of T cell infiltration was found between vehicle- and NOD-treated groups, albeit that in RT analysis a trend towards a reduced number of T cells in NOD-treated rats was observed (p=0.09, Figure 3B). Similarly, there was no difference between the groups with regard to macrophage infiltration (Figure 3D).

NOD inhibits proliferation and apoptosis of SMC in vitro

Since proliferation (in NI) and apoptosis (in media) of SMC are critical events in NI formation we further investigated the influence of NOD on these parameters *in vitro* using cultured haSMC as described in the *Methods* section. Proliferation was assessed after 48 hours of stimulation and showed a clear inhibition by NOD (Figure 4A). Cell cycle analysis revealed accumulation of cells in the G1-phase (Figure 4B) suggesting that cell cycle progression was reduced by NOD. G1-arrest was further substantiated by qPCR, showing a significant decrease in mRNA expression of *AURKA*, *CCNA2*, *CCNB1* and *CDK1*, genes known to be involved in G1-progression (Figure 4C).

In addition to its effect on cell proliferation, it was also found that NOD inhibited TNF-α-mediated SMC apoptosis. While in the absence of NOD approximately 13% of SMC already expressed Annexin V after 6 hours of TNF-α stimulation (p<0.001 *vs.* medium), in the presence of NOD this was significantly reduced (p<0.001 *vs.* no NOD, Figure 4D+E). The percentage of necrotic or late apoptotic $7AAD^+$ cells was not significantly different between all three groups.

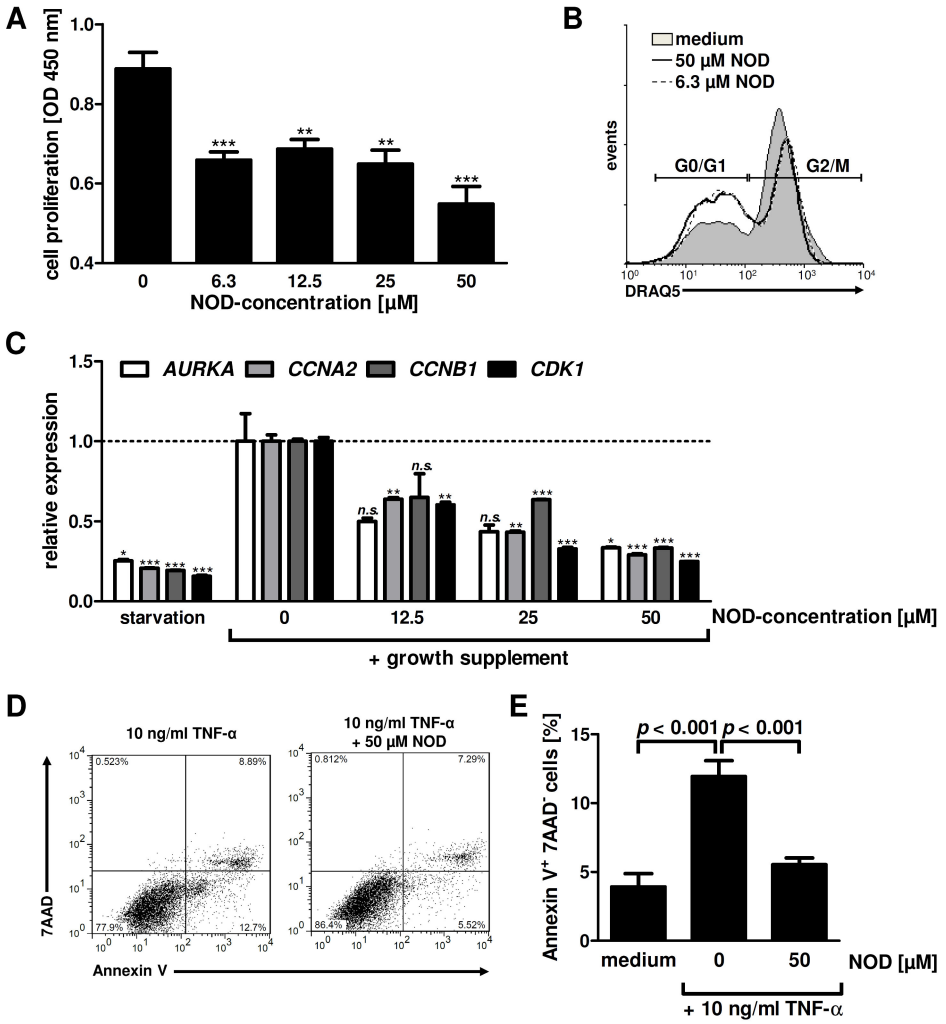

Figure 4: NOD inhibits proliferation and TNF-α-induced apoptosis in cultured haSMC.

A: haSMC were grown for 48 hours in the presence of different NOD-concentrations. Proliferation was assessed using the WST-1 proliferation assay. The results of a representative experiment are depicted as mean OD450 ± SEM of 6 replicate wells for each condition. A total of 4 independent experiments were performed (*n.s.* not significant).

B: haSMC were grown for 72 hours in the presence of different NOD-concentrations. Nuclei were stained with DRAQ5 and nuclear volume was assessed by FACS. Histogram shows the G0/G1 and G2/M peaks.

C: haSMC were grown for 72 hours in the presence or absence of different concentrations of NOD. mRNA was isolated and expression of cell cycle specific genes was assessed by qPCR. A total of 2 experiments in triplicate with essentially same results were performed (*n.s.* not significant, **p*<0.05, ***p*<0.01, ****p*<0.001 *vs.* 0 µM NOD).

D: haSMC were stimulated for 6 hours with 10 ng/ml TNF-α in the presence or absence of 50 µM NOD. Cells grown in medium (no TNF-α and NOD) served as control to assess baseline apoptosis. Apoptotic cells were defined as Annexin $V^+/7AAD^-$ cells, while necrotic or late apoptotic cells were defined as Annexin $V^+/7AAD^+$ double positive cells. Representative dot-plots are depicted.

E: Quantification of apoptotic cells from 4 independent experiments.

Discussion

Inasmuch as *in vitro* studies have indicated that NOD inhibits the expression of endothelial cell adhesion molecules, leukocyte adhesion to the endothelium [33] and T cell activation [34], the present study was conducted to assess if NOD has therapeutic efficacy to reduce TV in a model of allogeneic aorta transplantation in rats. The following two major findings were obtained in this study. Firstly, NOD significantly attenuated NI formation assessed 4 weeks after transplantation. Although this was associated with a reduction in the number of neointimal αSMA$^+$ cells, the proliferative state of these cells *in situ* was not affected. NOD-treatment did not abrogate vascular inflammation to a large extent, albeit that in NOD-treated rats the number of T cells in the adventitia was slightly decreased. Secondly, *in vitro* studies revealed that NOD inhibits proliferation and TNF-α-mediated apoptosis of haSMC. Inhibition of proliferation appeared to be mediated via a G1-arrest.

Although this study shows a clear therapeutic benefit of NOD to reduce NI formation in aortic allografts, it does not unequivocally demonstrate the molecular mechanism by which this occurs. Our *in vitro* data clearly showed that NOD inhibits SMC proliferation, yet this could not be confirmed *in situ* as proliferation (based on Ki67 expression) of αSMA$^+$ neointimal cells was not affected by NOD. It could be argued that Ki67, a well-established proliferation marker expressed in the G1-phase [38], might still be present despite the fact that cells cannot enter the S-phase [39]. However, also the expression of PCNA in αSMA$^+$ cells was not significantly different between the groups, suggesting that the αSMA$^+$Ki67$^+$ double positive cells were able to enter the S-phase. Yet, the number of αSMA$^+$ cells in the NI of aortic allografts obtained from NOD-treated rats was significantly reduced as compared to that of grafts obtained from vehicle-treated rats. This raises the question as to whether recruitment of hematopoietic progenitor cells or their differentiation into smooth muscle-like cells was affected by NOD. It should be mentioned in this regard that there is still ongoing controversy on the origin of SMC that populate the NI as both graft-derived and blood borne progenitor cells may have this propensity [14,40]. However, in experimental transplant models for TV in which no immunosuppression is used, graft-derived progenitor cells may be destroyed by alloreactive T cells and thus host cells may dominate repopulation of the decellularized vessel scaffold [41]. Thus far, there is no direct experimental evidence that NOD impairs progenitor cell recruitment.

We previously described a strong anti-inflammatory effect of NOD on endothelial cells [33] and T cells [34]. These observations were not confirmed in the current study as NOD did not influence the degree of infiltrated T cells and macrophages *in vivo*. However, only limited data is available for bioavailability and pharmacokinetics of NOD *in vivo*, and concentrations achieved *in vivo* might be far below from the concentrations used *in vitro* resulting in different cellular effects.

Beside cellular inflammation also cytokines are recognized to play a pivotal role in vascular inflammation. The relevance of cysteinyl leukotrienes (*i.e.* LTC4, LTD4) in the pathogenesis of atherosclerosis was first suggested by Porreca *et al.* in a model of balloon catheter injury of the carotid artery in rats, where it was shown that a leukotriene D4 receptor antagonist provided effective inhibition of neointimal thickening [42]. More recent studies have further supported the role of leukotrienes in the pathogenesis of neointimal hyperplasia [43-45]. Endogenous N-acyl-dopamines not only display anti-inflammatory and immunomodulatory activities due to their propensity to inhibit NF-κB regulated gene expression [33,46], they were initially described as potent inhibitors of 5-lipoxygenase [47]. Although the synthetic N-acyl-dopamine NOD shares a number of biological activities with endogenous ones, further studies are warranted to assess if NOD also inhibits 5-lipoxygenase and if this may explain its beneficial effect on TV in addition to its direct effects on SMC.

Apoptosis of medial SMC has been identified as amplifier for the development of TV as inhibition of SMC apoptosis was associated with a reduced NI formation [6]. *In vitro*, NOD was able to suppress TNF-α-induced apoptosis, yet *in vivo*, loss of medial αSMA expression was noticed in aortic allografts from both untreated and NOD-treated rats. However, loss of αSMA expression could be linked to phenotypic modulation and not necessarily to apoptosis. Chin *et al.* showed that metformin reduces I/R-injury and TV and suggested an AMP-activated protein kinase (AMPK) dependent mechanism that results in a lower apoptosis rate. We recently demonstrated that NOD activates AMPK [48], yet both NOD and metformin can act as antioxidants [49] and therefore this precludes drawing firm conclusions as to whether the anti-apoptotic effect of both compounds are exclusively mediated via AMPK activation.

In conclusion we demonstrate that NOD has a therapeutic efficacy to reduce NI formation in a rat model of allogeneic aorta transplantation. Our *in vitro* data clearly support anti-apoptotic and anti-proliferative effects of NOD on SMC. It remains to be shown that these beneficial effects of NOD are solely responsible for the protective *in vivo* effects on the development of TV.

Acknowledgements

We thank Dr. Annemieke Smit-van Oosten, Bianca Meijeringh and Michel Weij for their technical support with aortic transplantation, Marian Bulthuis for assistance with tissue processing and Annette Breedijk for her help with qPCR analyses. N-octanoyl-dopamine was kindly provided by Novaliq GmbH, Heidelberg, Germany. Sonja Theisinger and Bastian Theisinger (both Novaliq GmbH, Heidelberg, Germany) are acknowledged for scientific advice and technical assistance in formulation of N-octanoyl-dopamine.

References

1. Hong JC, Kahan BD (2000) Immunosuppressive agents in organ transplantation: past, present, and future. Semin Nephrol 20: 108-125.
2. Nankivell BJ, Borrows RJ, Fung CL, O'Connell PJ, Allen RD, et al. (2003) The natural history of chronic allograft nephropathy. N Engl J Med 349: 2326-2333.
3. Chapman JR, O'Connell PJ, Nankivell BJ (2005) Chronic renal allograft dysfunction. J Am Soc Nephrol 16: 3015-3026.
4. Mitchell RN, Libby P (2007) Vascular remodeling in transplant vasculopathy. Circ Res 100: 967-978.
5. Kouwenhoven EA, JN IJ, de Bruin RW (2000) Etiology and pathophysiology of chronic transplant dysfunction. Transpl Int 13: 385-401.
6. Zheng Q, Liu S, Song Z (2011) Mechanism of arterial remodeling in chronic allograft vasculopathy. Front Med 5: 248-253.
7. Sata M, Saiura A, Kunisato A, Tojo A, Okada S, et al. (2002) Hematopoietic stem cells differentiate into vascular cells that participate in the pathogenesis of atherosclerosis. Nat Med 8: 403-409.
8. George J, Afek A, Abashidze A, Shmilovich H, Deutsch V, et al. (2005) Transfer of endothelial progenitor and bone marrow cells influences atherosclerotic plaque size and composition in apolipoprotein E knockout mice. Arterioscler Thromb Vasc Biol 25: 2636-2641.
9. Langer HF, Chavakis T (2009) Leukocyte-endothelial interactions in inflammation. J Cell Mol Med 13: 1211-1220.
10. Gawaz M, Brand K, Dickfeld T, Pogatsa-Murray G, Page S, et al. (2000) Platelets induce alterations of chemotactic and adhesive properties of endothelial cells mediated through an interleukin-1-dependent mechanism. Implications for atherogenesis. Atherosclerosis 148: 75-85.
11. Kirk AD, Morrell CN, Baldwin WM, 3rd (2009) Platelets influence vascularized organ transplants from start to finish. Am J Transplant 9: 14-22.
12. Massberg S, Konrad I, Schurzinger K, Lorenz M, Schneider S, et al. (2006) Platelets secrete stromal cell-derived factor 1alpha and recruit bone marrow-derived progenitor cells to arterial thrombi in vivo. J Exp Med 203: 1221-1233.
13. Rabelink TJ, de Boer HC, van Zonneveld AJ (2010) Endothelial activation and circulating markers of endothelial activation in kidney disease. Nat Rev Nephrol 6: 404-414.
14. Hillebrands JL, Onuta G, Rozing J (2005) Role of progenitor cells in transplant arteriosclerosis. Trends Cardiovasc Med 15: 1-8.
15. Zhang LN, Wilson DW, da Cunha V, Sullivan ME, Vergona R, et al. (2006) Endothelial NO synthase deficiency promotes smooth muscle progenitor cells in association with upregulation of stromal cell-derived factor-1alpha in a mouse model of carotid artery ligation. Arterioscler Thromb Vasc Biol 26: 765-772.
16. Libby P, Pober JS (2001) Chronic rejection. Immunity 14: 387-397.
17. Ma X, Hibbert B, White D, Seymour R, Whitman SC, et al. (2008) Contribution of recipient-derived cells in allograft neointima formation and the response to stent implantation. PLoS One 3: e1894.
18. Song Z, Li W, Zheng Q, Shang D, Shu X, et al. (2007) The origin of neointimal smooth muscle cells in transplant arteriosclerosis from recipient bone-marrow cells in rat aortic allograft. J Huazhong Univ Sci Technolog Med Sci 27: 303-306.
19. Thyberg J, Blomgren K, Roy J, Tran PK, Hedin U (1997) Phenotypic modulation of smooth muscle cells after arterial injury is associated with changes in the distribution of laminin and fibronectin. J Histochem Cytochem 45: 837-846.
20. Rose ML (2007) Interferon-gamma and intimal hyperplasia. Circ Res 101: 542-544.

21. Hamano K, Bashuda H, Ito H, Shirasawa B, Okumura K, et al. (2000) Graft vasculopathy and tolerance: does the balance of Th cells contribute to graft vasculopathy? J Surg Res 93: 28-34.
22. Ueland T, Sikkeland LI, Yndestad A, Eiken HG, Holm T, et al. (2003) Myocardial gene expression of inflammatory cytokines after heart transplantation in relation to the development of transplant coronary artery disease. Am J Cardiol 92: 715-717.
23. Hart-Matyas M, Nejat S, Jordan JL, Hirsch GM, Lee TD (2010) IFN-gamma and Fas/FasL pathways cooperate to induce medial cell loss and neointimal lesion formation in allograft vasculopathy. Transpl Immunol 22: 157-164.
24. Zhang Y, Zong HT, Yang CC, Zhang XD (2011) The clinical implication of inhibiting platelet activation on chronic renal allograft dysfunction: a prospective cohort study. Transplant Proc 43: 2596-2600.
25. Denton MD, Davis SF, Baum MA, Melter M, Reinders ME, et al. (2000) The role of the graft endothelium in transplant rejection: evidence that endothelial activation may serve as a clinical marker for the development of chronic rejection. Pediatr Transplant 4: 252-260.
26. Eisen H, Kobashigawa J, Starling RC, Valantine H, Mancini D (2005) Improving outcomes in heart transplantation: the potential of proliferation signal inhibitors. Transplant Proc 37: 4S-17S.
27. Stadlbauer TH, Wagner AH, Holschermann H, Fiedel S, Fingerhuth H, et al. (2008) AP-1 and STAT-1 decoy oligodeoxynucleotides attenuate transplant vasculopathy in rat cardiac allografts. Cardiovasc Res 79: 698-705.
28. Schnuelle P, Gottmann U, Hoeger S, Boesebeck D, Lauchart W, et al. (2009) Effects of donor pretreatment with dopamine on graft function after kidney transplantation: a randomized controlled trial. JAMA 302: 1067-1075.
29. Benck U, Hoeger S, Brinkkoetter PT, Gottmann U, Doenmez D, et al. (2011) Effects of donor pre-treatment with dopamine on survival after heart transplantation: a cohort study of heart transplant recipients nested in a randomized controlled multicenter trial. J Am Coll Cardiol 58: 1768-1777.
30. Yard B, Beck G, Schnuelle P, Braun C, Schaub M, et al. (2004) Prevention of cold-preservation injury of cultured endothelial cells by catecholamines and related compounds. Am J Transplant 4: 22-30.
31. Losel RM, Schnetzke U, Brinkkoetter PT, Song H, Beck G, et al. (2010) N-octanoyl dopamine, a non-hemodyanic dopamine derivative, for cell protection during hypothermic organ preservation. PLoS One 5: e9713.
32. Ait-Hsiko L, Kraaij T, Wedel J, Theisinger B, Theisinger S, et al. (2012) N-octanoyl-dopamine is a potent inhibitor of platelet function. Platelets.
33. Hottenrott MC, Wedel J, Gaertner S, Stamellou E, Kraaij T, et al. (2013) N-octanoyl dopamine inhibits the expression of a subset of kappaB regulated genes: potential role of p65 Ser276 phosphorylation. PLoS One 8: e73122.
34. Wedel J, Hottenrott MC, Stamellou E, Breedijk A, Tsagogiorgas C, et al. (2014) N-Octanoyl dopamine transiently inhibits T cell proliferation via G1 cell-cycle arrest and inhibition of redox-dependent transcription factors. J Leukoc Biol.
35. Tsagogiorgas C, Wedel J, Hottenrott M, Schneider MO, Binzen U, et al. (2012) N-octanoyl-dopamine is an agonist at the capsaicin receptor TRPV1 and mitigates ischemia-induced acute kidney injury in rat. PLoS One 7: e43525.
36. Wedel J, Weij M, Oosten AS, Hillebrands JL (2014) Simultaneous subcutaneous implantation of two osmotic minipumps connected to a jugular vein catheter in the rat. Lab Anim.
37. Onuta G, van Ark J, Rienstra H, Boer MW, Klatter FA, et al. (2010) Development of transplant vasculopathy in aortic allografts correlates with neointimal smooth muscle cell proliferative capacity and fibrocyte frequency. Atherosclerosis 209: 393-402.

38. Gerdes J, Schwab U, Lemke H, Stein H (1983) Production of a mouse monoclonal antibody reactive with a human nuclear antigen associated with cell proliferation. Int J Cancer 31: 13-20.
39. van Dierendonck JH, Keijzer R, van de Velde CJ, Cornelisse CJ (1989) Nuclear distribution of the Ki-67 antigen during the cell cycle: comparison with growth fraction in human breast cancer cells. Cancer Res 49: 2999-3006.
40. Hillebrands JL, Klatter FA, van den Hurk BM, Popa ER, Nieuwenhuis P, et al. (2001) Origin of neointimal endothelium and alpha-actin-positive smooth muscle cells in transplant arteriosclerosis. J Clin Invest 107: 1411-1422.
41. Hillebrands JL, Klatter FA, Rozing J (2003) Origin of vascular smooth muscle cells and the role of circulating stem cells in transplant arteriosclerosis. Arterioscler Thromb Vasc Biol 23: 380-387.
42. Porreca E, Di Febbo C, Di Sciullo A, Angelucci D, Nasuti M, et al. (1996) Cysteinyl leukotriene D4 induced vascular smooth muscle cell proliferation: a possible role in myointimal hyperplasia. Thromb Haemost 76: 99-104.
43. Blazevic T, Schaible AM, Weinhaupl K, Schachner D, Nikels F, et al. (2014) Indirubin-3'-monoxime exerts a dual mode of inhibition towards leukotriene-mediated vascular smooth muscle cell migration. Cardiovasc Res 101: 522-532.
44. Gonzalez-Cobos JC, Zhang X, Zhang W, Ruhle B, Motiani RK, et al. (2013) Store-independent Orai1/3 channels activated by intracrine leukotriene C4: role in neointimal hyperplasia. Circ Res 112: 1013-1025.
45. Yu Z, Ricciotti E, Miwa T, Liu S, Ihida-Stansbury K, et al. (2013) Myeloid cell 5-lipoxygenase activating protein modulates the response to vascular injury. Circ Res 112: 432-440.
46. Sancho R, Macho A, de La Vega L, Calzado MA, Fiebich BL, et al. (2004) Immunosuppressive activity of endovanilloids: N-arachidonoyl-dopamine inhibits activation of the NF-kappa B, NFAT, and activator protein 1 signaling pathways. J Immunol 172: 2341-2351.
47. Tseng CF, Iwakami S, Mikajiri A, Shibuya M, Hanaoka F, et al. (1992) Inhibition of in vitro prostaglandin and leukotriene biosyntheses by cinnamoyl-beta-phenethylamine and N-acyldopamine derivatives. Chem Pharm Bull (Tokyo) 40: 396-400.
48. Stamellou E, Fontana J, Wedel J, Ntasis E, Sticht C, et al. (2014) N-octanoyl dopamine treatment of endothelial cells induces the unfolded protein response and results in hypometabolism and tolerance to hypothermia. PLoS One 9: e99298.
49. Hou X, Song J, Li XN, Zhang L, Wang X, et al. (2010) Metformin reduces intracellular reactive oxygen species levels by upregulating expression of the antioxidant thioredoxin via the AMPK-FOXO3 pathway. Biochem Biophys Res Commun 396: 199-205.